Wave mode conversion and mode transition in very high radio frequency helicon plasma

G. S. Eom, Junghee Kim, and W. Choe[a)]
Department of Physics, Korea Advanced Institute of Science and Technology, 373-1 Guseong-dong, Yuseong-gu, Daejeon 305-701, Korea

(Received 7 November 2005; accepted 22 June 2006; published online 21 July 2006)

In a very high radio frequency helicon plasma, experimental evidences for a wave mode conversion between the helicon mode and the Trivelpiece-Gould mode (TG mode) are presented. The helicon mode generation was detected when $\omega < \omega_{ce}/2$ was satisfied, and the helicon mode was converted to the TG mode at the plasma periphery below 140 G. As no more mode conversion to the TG mode occurs above 140 G, the plasma was directly heated by the helicon mode and a subsequent abrupt mode transition occurred. © *2006 American Institute of Physics*. [DOI: 10.1063/1.2226981]

I. INTRODUCTION

Since the first report of efficient plasma heating with the helicon wave, the helicon wave discharges have been studied intensively due to its efficient plasma generation with the low rf power density.[1–3] The helicon plasmas have been generated in the frequency range of $\omega_{ci} \ll \omega < \omega_{ce} \ll \omega_{pe}$.[1–4] Many previous results asserted that the power absorption in the helicon plasma is due to the Trivelpiece-Gould mode (TG mode).[5–8] Although many researchers have been trying to explain the mechanisms of efficient power absorption, it has not been clearly examined yet due to difficulties in its detection.[5,9] As the TG mode tends to be localized in a thin surface layer, the direct measurement is too difficult. Due to the difficulty of measurement, almost no experimental evidence for the heating by the TG mode has been reported. In the experiment performed by Blackwell *et al.*,[10] the axial current profile of TG mode was presented in a comparison to the theoretical prediction.[7] Although it provides evidence for the existence of the TG mode, it did not directly show that the TG mode is absorbed in the plasma periphery.

Meanwhile, Shamrai and Taranov theoretically proposed that the mode conversion from the helicon mode to the TG mode plays a significant role in the plasma heating.[5] For $\omega \ll \omega_{ce}$, the wave dispersion is separated into two wave modes, namely the helicon mode and the TG mode. They report that those two wave modes merge under a typical condition and that the helicon mode converts to the TG mode. Subsequently, in an inhomogeneous plasma, the converted TG mode electrostatically oscillates at the plasma periphery and heats up the plasma.[11]

By showing the existence of TG modes and the power absorption by the TG mode in a very high radio frequency (VHF) helicon plasma, we report the experimental observations in this article, indicating that the $H-W$ mode transition occurs due to the changed role of helicon mode and TG mode. In the case of 98 MHz at which the helicon plasma was produced, an external magnetic field for the electron cyclotron resonance to occur corresponds to approximately 35 G, which leads to $\omega_{ci} \ll \omega < \omega_{ce} \ll \omega_{pe}$, where ω_{ci}, ω_{ce}, and ω_{pe} are ion cyclotron frequency, electron cyclotron frequency, and electron plasma frequency, respectively. Therefore, the displacement current in the well-known whistler dispersion relation was taken into account.

II. EXPERIMENTAL APPARATUS

A schematic diagram of helicon plasma source used for the experiment is shown in Fig. 1. The discharge tube was 5 cm in diameter and 30 cm in length and was connected to a multiport diagnostic chamber. A turbomolecular pump and a mechanical pump were connected to the diagnostic chamber to provide a base pressure as low as 10^{-7} Torr. Eight electrical coils generated an axial magnetic field from $z=0$ (center of the discharge tube) to $z=\pm 9$ cm in the (r, θ, z) cylindrical coordinates. The maximum magnetic field produced was 800 G with less than 2% field ripple. The magnetic field was swept by the external trigger signal of triangle function, which made the continuous data acquisition and the sweeping frequency control possible. The frequency of the rf generator used in the experiment was 98 MHz with a variable power of up to 100 W. Plasmas were produced by using a silver-coated Nagoya Type III antenna to reduce the antenna resistance. The antenna length and diameter were 3.5 and 5.5 cm, respectively.

As shown in Fig. 1, a double B-dot probe was placed in the axial direction to measure the wave number. A detailed hardware setup for the phase diagnostics in the heterodyne scheme is described in Ref. 12. The detection of Ar II emission intensity was carried out in the direction of external magnetic field using a charge coupled device camera and a 488 nm Ar II optical filter. Once the line-integrated (in the z direction) two-dimensional (in r and θ) image was pictured, the spatial Ar II emission intensity at a fixed z position was obtained by correcting the signal in consideration of the viewing angle and the focal length of the camera.

III. RESULTS AND DISCUSSIONS

The radially line-averaged plasma density by using the planar Langmuir probe versus the external magnetic field is

[a)]Author to whom correspondence should be addressed. Electronic mail: wchoe@kaist.ac.kr

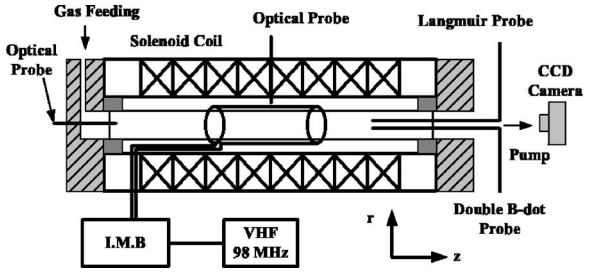

FIG. 1. Schematic diagram of helicon plasma source used for the experiments. A Nagoya Type III antenna is seen.

shown in Fig. 2. The plasma density was scanned between two antenna legs at intervals of 0.5 mm [Fig. 3(a)] and then averaged. The wave mode transition was occurred at 140 G as mentioned in our previous paper[13] and the plasma density was decreased for a while. In a radial direction, Figs. 3(a) and 3(b) also show a distinct difference of those two cases. It appears as if the inductive heating and the wave heating are related before and after the transition as common reports on the helicon wave launch,[3,14] but further research shows that this transition is not due to the inductive-to-wave transition.

The Ar II emission intensity in the helicon plasma is known to be proportional to the square of the plasma density,[15] and is given by

$$I \propto \langle \sigma v \rangle n_e^2, \tag{1}$$

where σ is the cross section and $\langle \sigma v \rangle$ is the excitation rate coefficient of 488 nm Ar^+ emission. Figure 3(c) shows the excitation rate coefficients at three different external field conditions with a reference excitation rate coefficient under the common inductively coupled condition, which was obtained by substituting the measured density profile [Fig. 3(a)] and the 488 nm Ar II emission intensity [Fig. 3(b)] into Eq. (1). It is considered that the four orders of magnitude in the $\langle \sigma v \rangle$ curve at the plasma periphery shown in Fig. 3(c) is in some sense exaggerated because of the following two reasons: first, n_e at the plasma periphery is much smaller than that of the core region so that a measurement error at the plasma boundary may bring about a large value of $\langle \sigma v \rangle$ because $\langle \sigma v \rangle \propto 1/n_e^2$. Second, the discretely measured n_e was fitted to a polynomial function of r for calculating $\langle \sigma v \rangle$ using Eq. (1) as one of the helicon plasma properties. An uncertainty at the plasma boundary in the fitting function may

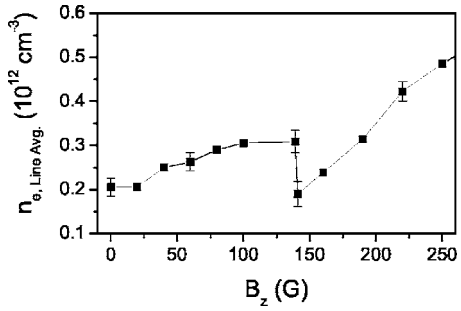

FIG. 2. Radially line-averaged plasma density as external field. Plasma density between two antenna legs was averaged: argon, 1.5 mTorr and 65 W.

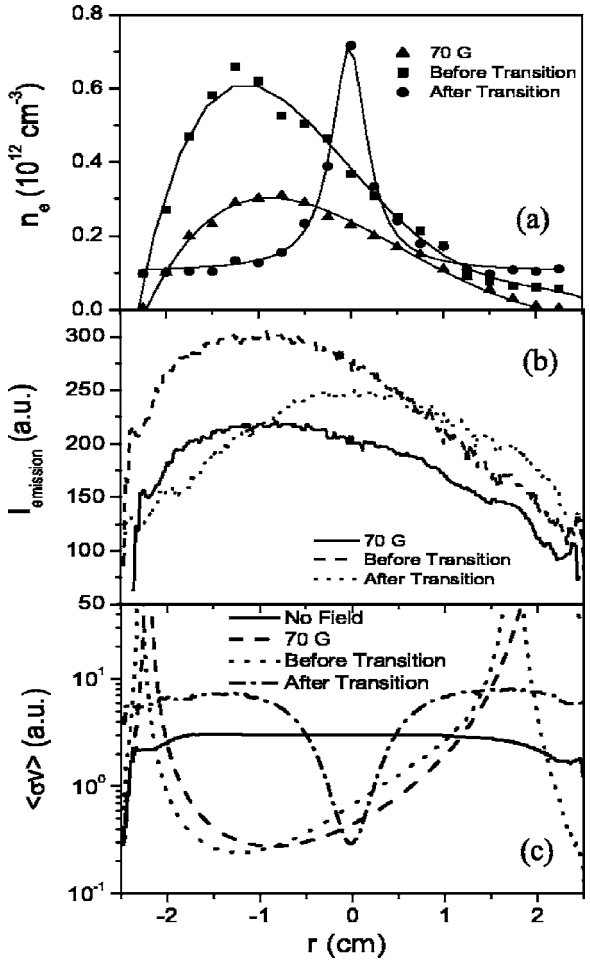

FIG. 3. Radial profiles of (a) the measured plasma density, (b) the measured 488 nm Ar II emission intensity, and (c) the excitation rate coefficient $\langle \sigma v \rangle$. In the legends, before transition is just below 140 G and after transition is just above 140 G; argon, 1.5 mTorr and 65 W.

cause a large peak of $\langle \sigma v \rangle$ by the same reason. It is noted that despite the somewhat inaccurate value of $\langle \sigma v \rangle$ at the plasma boundary, a distinctive difference is seen in $\langle \sigma v \rangle$ profile with respect to $B_z \approx 140$ G before and after the transition. Before the transition at 140 G, the peak of $\langle \sigma v \rangle$ was localized near the antenna legs. However, after the transition ($B_z > 140$ G), the localized peak near the antenna leg was disappeared, on the other hand, $\langle \sigma v \rangle$ showed an entirely different profile compared to the case of "before the transition." In Fig. 3(c), a coupled peak near the antenna leg was appeared for both cases of 70 G and "before transition." However, it is also seen that $\langle \sigma v \rangle$ is slightly shifted toward one of the legs; This slight asymmetry over the two antenna legs is considered to be due to the remained nonuniform inductive coupling commonly occurring in the VHF inductively coupled plasma devices along the antenna.[16] In the case of "after transition," $\langle \sigma v \rangle$ was decreased at the radial center, because of the increased plasma density due to a very active ionization which is generally accepted as one of helicon plasma properties.

To interpret the experimental results, the following well-known whistler wave dispersion relation is considered[9]:

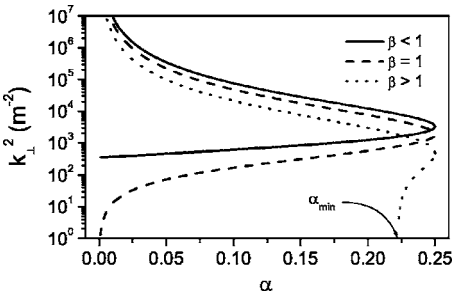

FIG. 4. $k_\perp^2$ plotted against α.

$$\frac{k^2c^2}{\omega^2} = 1 - \frac{\omega_{pe}^2}{\omega(\omega\gamma - \omega_{ce}\cos\theta)}, \tag{2}$$

where $k=\sqrt{k_\parallel^2+k_\perp^2}$ is the squared total wave number, $\cos\theta = k_\parallel/k$, $\gamma=1+i(\nu/\omega)$, and ν are the frequency of electron collisions with neutrals and ions. In the case of $\nu=0$, $\cos\theta=1$ ($\theta\ll1$), and $\omega\ll\omega_{ce}$, Eq. (2) is approximately resolved as a biquadratic equation derived by Shamrai and Taranov as follows[6]:

$$k_{\perp\pm}^2 = k_\parallel^2\frac{1}{2\alpha^2\beta^2}(1-2\alpha-2\alpha^2\beta^2 \pm \sqrt{1-4\alpha}), \tag{3}$$

where $\alpha=(\omega_{pe}^2\omega^2)/(\omega_{ce}^2k_\parallel^2c^2)$ and $\beta=(\omega\omega_{ce}k_\parallel^2c^2)/(\omega_{pe}^2\omega^2)$. In Eq. (3), + and − signs correspond to the TG mode and the helicon mode, respectively. As ω is near ω_{ce} in our experimental circumstances, the displacement current can no longer be ignored. Using the measured $k_\parallel$, applied B field, and n_e, the plot of $k_\perp^2$ versus α shown in Fig. 4 was obtained from Eq. (2) with the displacement current term taken into account. It is well known that the propagating electromagnetic wave (helicon mode) is converted to the electrostatic resonance (TG mode) when the two waves are merged at $\alpha=1/4$(i.e., $k_{\perp-}^2=k_{\perp+}^2$) as seen in Fig. 4.[6,17] In our experiment, the corresponding plasma density for the merge of the two waves is approximately 1.8×10^{10} cm^{-3} at 70 G. As α is larger than 1/4 above this plasma density, the two waves can be merged only at the plasma periphery. The measured plasma density was approximately 10^{10} cm^{-3} at the sheath-to-plasma boundary. As α approached 1/4, $k_{\perp-}$ and $k_{\perp+}$ became complex conjugates of each other ($k_{\perp-}=43.4+i3.81$ and $k_{\perp+}=43.4-i3.81$ in this experiment). Upon considering $E_r\propto\exp\{i(k_\perp r-\omega t)\}$, the electromagnetic field (helicon mode) was steeply and spatially damped out at $\alpha=1/4$, but the electrostatic field (TG mode) steeply grew in the radial direction, which indicate that the electromagnetic wave energy was converted to the electrostatic wave energy. After all, the steep ionization localized at the plasma periphery occurred from the steeply grown electrostatic field, resulting in a surface resonance.

Figure 5 shows the measured parallel wave number as a function of the external magnetic field and the radially integrated 488 nm Ar II emission line intensity. As seen in Fig. 5, a small peak in the Ar II emission intensity appeared near 35 G, which is the same magnetic field with the electron cyclotron resonance (ECR) at 98 MHz. The corresponding peaks at other frequencies were also appeared at ECR conditions (e.g., 65 G at 180 MHz). To classify the helicon wave component and the rf component radiated from the antenna, the rf component from the rf generator was used as an external trigger and the signal from a single B-dot probe was monitored as shown in Fig. 6. In Fig. 6, the trigger signal level was adjusted to the B-dot probe signal for an easy comparison. Off-phasing of the signal was detected at 70 G which corresponds to $\omega_{ce}/2$ and did not depend on the RF power, the gas pressure, or the cavity length. This indicates the limitation of helicon wave propagation at $\omega<\omega_{ce}/2$.[9] Above 70 G ($\omega<\omega_{ce}/2$), however, strong surface ionization was occurred as shown in Fig. 3(c).

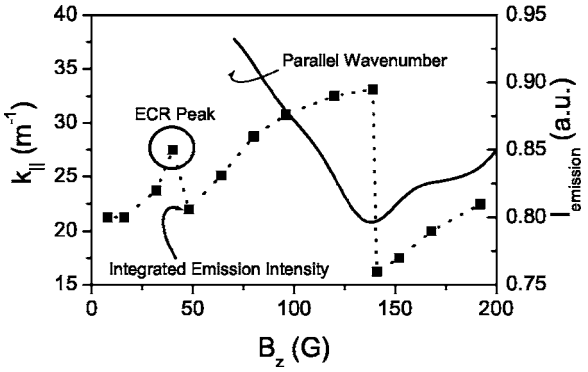

FIG. 5. Measured parallel wave number (straight line) plotted against B_z. The squared points connected by the dotted line present radially integrated 488 nm Ar II emission line intensity; argon, 1.5 mTorr and 65 W.

To investigate the relation between the plasma density, the parallel wave number, and the external magnetic field below 140 G, as the corresponding phenomena occur when $\alpha=1/4$ is satisfied, one can write the wave dispersion related to the mode conversion from the helicon mode to the TG mode as follows:

$$\frac{k_\parallel^2c^2}{\omega^2} = \frac{4\omega_{pe}^2}{\omega_{ce}^2} \propto \frac{n_e}{B_z^2}. \tag{4}$$

Since the plasma density did not vary significantly in the range from 70 to 140 G as shown in Fig. 2, the increase of B_z resulted in the decrease of $k_\parallel$ from Eq. (4). It agrees well with the measured $k_\parallel$ values in Fig. 5. For a low external field ($70<B_z<140$ G), dominant ionization occurred at the plasma periphery as a result of $k_{\perp-}^2=k_{\perp+}^2$, and $k_\parallel$ monotonically decreased as the external magnetic field was increased.

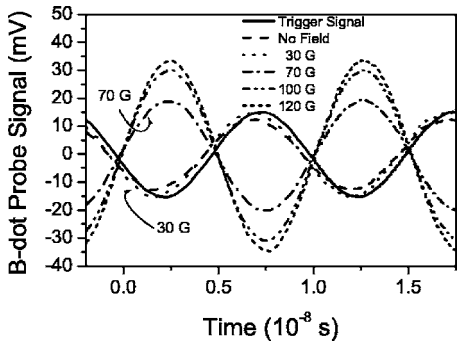

FIG. 6. Single B-dot probe signal; argon, 1.5 mTorr and 65 W.

Above 140 G, however, $k_{\parallel}$ increased, obeying the dispersion relation for the electromagnetic helicon wave.[1,2,4] After the mode transition occurs at 140 G, α was much lower than 1/4 in the bulk plasma, and there is no area satisfying the condition of $\alpha=1/4$ as α is inversely proportional to the square of the external magnetic field ($\alpha \propto n_e/(B_z^2 k_{\parallel}^2)$). Therefore, no more helicon-to-TG mode conversion occurred in the bulk plasma. When the mode transition occurred at 140 G, as the plasma column of the adjacent of antenna leg disappeared due to the sudden disappearance of the mode conversion, only the center core remained and plasma density had a sudden deep in Fig. 2. It was strictly checked by lengthening the sweeping period of external field. From those results, it is convincing that the wave mode transition at 140 G originated in the mode transition from the surface mode (helicon-to-TG mode conversion) to the global-heating mode (helicon mode). In the case of after the transition, the surface heating suddenly disappeared and the power absorption occurred throughout the plasma directly by helicon mode, which resulted in an abrupt mode transition.

Although the direct heating by helicon wave occurred before the transition, its contribution was not significant compared to that by the TG mode which was converted from the helicon mode at the plasma periphery. One can evidently witness this from the low plasma density at the moment of mode transition in Figs. 2 and 3.

IV. CONCLUSIONS

We presented evidence that an abrupt wave mode transition in helicon plasma originated in the mode transition from the surface mode (helicon-to-TG mode conversion) to the global-heating mode (helicon mode). A small density peak observed near 35 G is due to the electron cyclotron resonance, and an off-phasing near $\omega=\omega_{ce}/2$ indicates the frequency criterion for the helicon wave to launch. Contrary to the understanding that the helicon mode launches when the abrupt jump of plasma density occurs, the helicon mode already exists only if $\omega<\omega_{ce}/2$ is satisfied as estimated by Chen.[9] In the plasma periphery satisfying the condition of $k_{\perp-}^2=k_{\perp+}^2$, the mode conversion from the helicon mode to the TG mode occurs. The converted TG mode plays a main role in the plasma heating before the transition. After the transition, however, the plasma heating by the mode conversion disappears, resulting in a direct heating by the helicon mode as the main mechanism for plasma heating. Although the direct heating by an antenna-produced TG mode is possible in consideration with many other theoretical predictions, in this paper we show experimental evidence that helicon-to-TG mode conversion plays a dominant role in plasma heating before the transition in a VHF plasma. Conclusively the abrupt plasma density jump and the mode transition at 140 G occurs due to the changed heating mechanism between helicon mode and TG mode.

ACKNOWLEDGMENT

The authors thank Dr. Suwon Cho for careful reading and useful discussions. This work was supported by the Ministry of Commerce, Industry and Energy of the Republic of Korea.

[1] R. W. Boswell, Plasma Phys. Controlled Fusion **26**, 1147 (1984).
[2] F. F. Chen, Plasma Phys. Controlled Fusion **33**, 339 (1991).
[3] F. F. Chen, J. Vac. Sci. Technol. A **10**, 1389 (1992).
[4] G. S. Eom, I. D. Bae, G. Cho, and W. Choe, Plasma Sources Sci. Technol. **10**, 417 (2001).
[5] K. P. Shamrai and V. B. Taranov, Plasma Phys. Controlled Fusion **36**, 1719 (1994).
[6] K. P. Shamrai and V. B. Taranov, Plasma Sources Sci. Technol. **5**, 474 (1996).
[7] D. Arnush, Phys. Plasmas **7**, 3042 (2000).
[8] Y. Mouzouris and J. E. Scharer, Phys. Plasmas **5**, 4253 (1998).
[9] F. F. Chen and D. Arnush, Phys. Plasmas **4**, 3411 (1997).
[10] D. D. Blackwell, T. G. Madziwa, D. Arnush, and F. F. Chen, Phys. Rev. Lett. **88**, 145002 (2002).
[11] A. V. Timofeev, Plasma Phys. Rep. **28**, 906 (2002).
[12] G. S. Eom, G. C. Kwon, I. D. Bae, G. Cho, and W. Choe, Rev. Sci. Instrum. **72**, 410 (2001).
[13] G. S. Eom and W. Choe, J. Vac. Sci. Technol. A **20**, 2079 (2002).
[14] A. J. Perry, D. Vender, and R. W. Boswell, J. Vac. Sci. Technol. B **9**, 310 (1991).
[15] D. D. Blackwell and F. F. Chen, Plasma Sources Sci. Technol. **6**, 569 (1997).
[16] K. Nakamura, K. Suzuki, and H. Sugai, Jpn. J. Appl. Phys., Part 1 **34**, 2152 (1995).
[17] T. H. Stix, *Waves in Plasmas* (AIP, New York, 1992), p. 339.